

Research Article

The Impact of Three Specific Collaborative Merging Strategies on Traffic Flow

Xue-Cheng Shang ^{1,2} Feng Liu ² Xin-Gang Li ¹ Davy Janssens,² and Geert Wets²

¹Key Laboratory of Transport Industry of Big Data Application Technologies for Comprehensive Transport, Beijing Jiaotong University, Beijing 100044, China

²Transportation Research Institute (IMOB), Hasselt University, Wetenschapspark 5, Bus 6, B-3590 Diepenbeek, Belgium

Correspondence should be addressed to Feng Liu; feng.liu@uhasselt.be and Xin-Gang Li; lixingang@bjtu.edu.cn

Received 24 July 2022; Revised 13 December 2022; Accepted 24 December 2022; Published 16 January 2023

Academic Editor: Jose E. Naranjo

Copyright © 2023 Xue-Cheng Shang et al. This is an open access article distributed under the Creative Commons Attribution License, which permits unrestricted use, distribution, and reproduction in any medium, provided the original work is properly cited.

On-ramps are considered to be one of the common traffic bottlenecks. In order to improve the operation efficiency of on-ramps, scholars worldwide have proposed various vehicle merging strategies. In this study, we designed different rules to express three collaborative strategies and studied their impact on on-ramp systems. Cellular automata models were used to simulate the systems under different situations, and the average speed and traffic flow rate of both the main roads and ramps were analyzed. The results show that (1) all the three merging strategies give excessive “priority” to the merging vehicle, leading to a severe reduction in the traffic performance of the main road; (2) nevertheless, these strategies have different effects on the entire system with a one-lane or two-lane main road. Due to the lane-changing behavior, the system with a two-lane main road has more advantages than that featured with a one-lane road, making the former system performing better than the latter under the same strategies; (3) the vehicles on the ramp and main road affect each other, and as the vehicle entering probabilities become large, the traffic flow rate on the main road decreases whereas that on the ramp increases. However, the effect is not unlimited, the flow rate on both roads finally reaches a stable level (forming a “platform”); and (4) large values of the merging safety distance parameter decrease the flow rate of the entire system. All the previous results provide a deep understanding of the impact of the three merging strategies on traffic flow, contributing to the design of on-ramp systems that have better operation efficiency and low levels of congestion.

1. Introduction

The rapid development of cities is bound to bring serious traffic problems (such as traffic congestion and traffic accidents), which will further lead to an adverse effect on economic development. In order to understand the evolution mechanism of traffic, various models have been proposed. Helbing [1] reviewed the major approaches to modeling vehicle traffic, including microscopic (particle-based), mesoscopic (gas-kinetic), and macroscopic (fluid-dynamic) models. Particularly, regarding microscopic models, Gipps [2] proposed a car-following model and used it to reproduce some characteristics of real traffic flow, while Nagel and Schreckenberg [3] constructed a basic cellular

automaton traffic flow model (i.e., the NaSch model). Moreover, Kerner and Rehborn [4, 5] developed the three-phase traffic flow theory based on real traffic observation data, and a number of similar models were put forward based on this theory [6, 7]. In addition, the rapid development of technology gave birth to the concept of intelligent vehicles (e.g., connected and autonomous vehicles), and such vehicles have entered specific markets. The vehicles can communicate with each other and cooperate to complete certain driving tasks (such as lane changing and collaborative merging) [8].

Traffic congestion often occurs on on-ramps, leading to the sections of roads being considered as one of the common traffic bottlenecks [9, 10]. Moreover, congestion can easily

spread to the upstream parts of the main roads and seriously affect the operation efficiency of the entire on-ramp systems (consisting of ramps and their connected acceleration lanes and main roads) [11]. Over the past decades, the study on on-ramps has attracted a lot of attention. From the initial phase diagrams [11, 12] to the later coordinated merging strategies [13, 14], various characteristics of on-ramp systems have been analyzed [12, 15], and methods to improve the traffic condition of the systems have been put forward [16, 17]. These studies can be divided into two major categories: optimization and simulation. Optimization is to design trajectories of vehicles with the goal of systematic or individual optimality in terms of certain traffic variables (e.g., flow rate, travel time, fuel consumption, and comfort levels) [18]. In comparison, simulation aims to mimic driving behavior or traffic rules in order to study the impact of the different behavior or rules on on-ramp systems. Particularly, cellular automata (CA) (microscopic) models are widely adopted to simulate traffic flow systems, because of the models' simple rules and easy implementation. From the classic single-lane NaSch traffic flow model [3] to the improved models [19–22], and to the two-lane [23, 24] or even multilane [25, 26] models, CA methods have demonstrated their value in well-depicting the characteristics of both microdriving behavior and macrosystem evolution. Based on the models, Campari and Levi [27], Zeng et al. [10], Jiang et al. [28], and Diedrich et al. [29] simulated on-ramp systems and investigated their evolution characteristics.

Alongside the micro simulation (by CA models), different merging strategies have been proposed [30–32] to devise vehicle driving behavior (e.g., vehicle acceleration or deceleration) at ramps, in order to facilitate the vehicle merging process and improve the traffic condition of on-ramp systems. Scarinci and Heydecker [17] summarized the major merging strategies and reviewed existing evaluation methods on the overall effect of the strategies. However, none of the existing studies have conducted comprehensive analysis and detailed comparison among strategies. To fill in this gap, this paper examines three representative collaborative merging strategies of connected and autonomous vehicles and analyses their impact on on-ramp systems by means of simulation methods (i.e., CA models). The core of these strategies proposes that vehicles on the main road provide “priority” condition for the merging vehicles on the acceleration lane (of the ramp) by the change of the speed of the former vehicles within capability ranges. In this analytical process, the three strategies are first expressed by the corresponding merging rules, and simulation is performed to reproduce the on-ramp system. The average speed and traffic flow rate of the roads in the system are then obtained, and the impact of these strategies is finally examined. The major contributions of this study lie in the following aspects: (1) it conducts a comparative analysis of the impact of different merging strategies on on-ramp systems, (2) it examines the influence of lane-changing behavior on the operation efficiency of the systems, and (3) it further investigates the effect of merging safety distances on the performance of the systems.

The remainder of this paper is organized as follows: Section 2 introduces the merging strategies and corresponding merging rules, while Section 3 describes the simulation process and analyses the simulation results. Finally, Section 4 ends this paper with a major conclusion and policy recommendation.

2. Merging Strategies and Update Rules

In this section, we first introduce the CA model and then give the definition of certain important variables. We further summarize the three collaborative merging strategies, and describe the update rules (including the merging rules) adopted in the CA model for simulating an on-ramp system.

2.1. The Cellular Automata (CA) Model. The CA model is a discrete model method in time and space first proposed by von Neumann [33] to simulate the self-replication function of living systems. It is a rule-based system evolution model, in which all individual objects in the system update their states (or positions) according to one or multiple rules. In the CA model for traffic flow, the entire road space is discretized into a set of cells, with each cell having two states including “empty” or “occupied (by a vehicle).” Rules (as described in Section 2.4) are formulated according to real driving behavior, and vehicles are updated according to the established rules to reflect the evolution process of the traffic flow system.

2.2. Variable Definition

Veh_m , the merging vehicle m on the acceleration lane;
 $Veh_{m,back2}$ and $Veh_{m,back1}$, the second and first (nearest) vehicles behind Veh_m on the main road, respectively;

$Veh_{m,front1}$ and $Veh_{m,front2}$, the first and second (nearest) vehicles in front of Veh_m on the main road, respectively;

x_m , $x_{m,back2}$, $x_{m,back1}$, $x_{m,front1}$ and $x_{m,front2}$, the position of Veh_m , $Veh_{m,back2}$, $Veh_{m,back1}$, $Veh_{m,front1}$, and $Veh_{m,front2}$, respectively;

v_m , $v_{m,back2}$, $v_{m,back1}$, $v_{m,front1}$ and $v_{m,front2}$, the velocity of Veh_m , $Veh_{m,back2}$, $Veh_{m,back1}$, $Veh_{m,front1}$, and $Veh_{m,front2}$, respectively;

Δt , the time step during which vehicles are updated in the CA model;

S^m , the traffic state array of Veh_m (defined in equation (1));

T^m , the threat array of Veh_m (defined in equation (2)).

Some notations are shown in Figure 1.

The state array S^m and threat array T^m of Veh_m are defined as follows [8]:

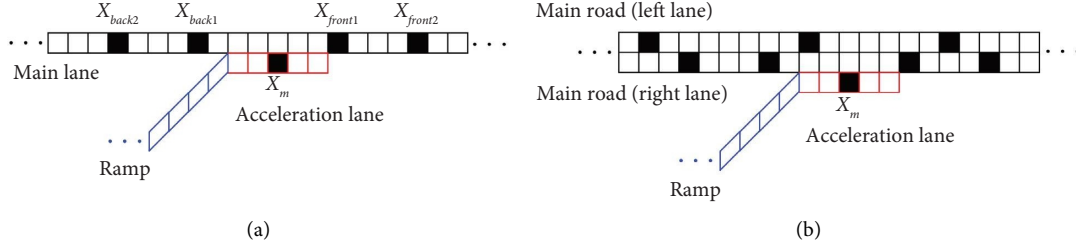


FIGURE 1: Schematic diagram of an on-ramp system with an (a) one-lane main road and (b) a two-lane main road.

$$S^m = [S_1^m, S_2^m, S_3^m, S_4^m, S_5^m] \\ = [x_{m,back2} + v_{m,back2} \cdot \Delta t, x_{m,back1} + v_{m,back1} \cdot \Delta t, x_m + v_m \cdot \Delta t, x_{m,front1} + v_{m,front1} \cdot \Delta t, x_{m,front2} + v_{m,front2} \cdot \Delta t], \quad (1)$$

$$T^m = [T_1^m, T_2^m] \\ = [S_3^m - S_2^m, S_4^m - S_3^m] - l - d_{safe,t} \\ = [S_3^m - S_2^m - l - d_{safe,t}, S_4^m - S_3^m - l - d_{safe,t}]. \quad (2)$$

In equation (1), S_i^m ($i = 1, \dots, 5$) is the i th element in S^m , while in equation (2), l is the vehicle length, $d_{safe,t}$ is the safety distance of merging strategies, and T_j^m ($j = 1, 2$) is the j th element in T^m . The state array S^m represents the position (S_3^m) of vehicle Veh_m as well as the positions (S_1^m, S_2^m, S_4^m and S_5^m) of the four nearest vehicles around Veh_m after a time step (Δt). The threat array T_j^m ($j = 1, 2$) refers to the relative distance (T_1^m) between Veh_m and $Veh_{m,back1}$ as well as the distance (T_2^m) between Veh_m and $Veh_{m,front1}$. The elements in T^m reflect whether Veh_m has a collision after Δt . When T_j^m ($j = 1, 2$) is greater than or equal to 0, no accident would occur; on the contrary, if T_j^m is smaller than 0, a collision is likely to happen.

2.3. Merging Strategies. Emulating the collaborative merging behavior of connected and autonomous vehicles, we consider three merging strategies, each of which ensures the safety of the merging vehicle and its surrounding vehicles. Equation (3) defines the safety condition when Veh_m merges into the main road.

$$T_1^m \geq 0, T_2^m \geq 0. \quad (3)$$

Combining equations (2) and (3), we obtain

$$S_3^m - S_2^m - l - d_{safe,t} \geq 0, S_4^m - S_3^m - l - d_{safe,t} \geq 0. \quad (4)$$

The first part of equation (4) shows that Veh_m will not be hit by $Veh_{m,back1}$ after merging, while the second part indicates that Veh_m will not strike $Veh_{m,front1}$ after merging. If equation (3) (or equation (4)) is satisfied, Veh_m will merge into the main road without risks of crash. However, when the safety condition is not met, the following strategies could be considered:

Strategy 1: $Veh_{m,front1}$ accelerates to provide safety condition for Veh_m

Strategy 2: $Veh_{m,back1}$ decelerates to provide safety condition for Veh_m

Strategy 3: $Veh_{m,front1}$ accelerates and $Veh_{m,back1}$ decelerates to provide safety condition for Veh_m

2.4. Update Rules. The rules for simulating an on-ramp system in the CA model include four parts: the rules for vehicles entering the main road or ramp, the forward rules for all vehicles, the lane changing rules for vehicles on the two-lane main road, and the merging rules for the merging vehicles.

2.4.1. Entry Rules. The same entry rules as those proposed in Reference [12] are considered. The on-ramp system adopts open boundary conditions, with the entrance on the left side of the main lane (or ramp) and the exit on the right side; see Figure 2(a). The leftmost cells of the road serve as the entry area, and the number of the cells covered by this area is $\Delta t \cdot v_{max}$ (the maximum velocity of vehicles). Let x_{last} be the location of the current leftmost vehicle on the main lane (or ramp) before each time step (Δt) update. If $x_{last} > v_{max} \cdot \Delta t$, a new vehicle will enter the position of $\min[x_{last} - v_{max} \cdot \Delta t, v_{max} \cdot \Delta t]$ on the main road (or ramp) with the probability of a_1 (or a_2).

2.4.2. Forward Rules. The forward rules are based on the traditional one-lane CA model, i.e., the NaSch model [3], which consists of acceleration (acceleration rate is $1 \text{ cell}/\Delta t^2$), deceleration (deceleration rate is $-1 \text{ cell}/\Delta t^2$), randomization, and position updating after a time step.

Step1: acceleration: $v_n \rightarrow \min(v_{max}, v_n + 1 \text{ cell}/\Delta t)$;

Step2: deceleration: $v_n \rightarrow \min(v_n, d_n/\Delta t)$;

Step3: randomization: $v_n \rightarrow \max(v_n - 1 \text{ cell}/\Delta t, 0)$ with probability p_s ;

Step4: position updating: $x_n \rightarrow x_n + v_n \cdot \Delta t$, where x_n and v_n denote the position and velocity of the subject vehicle (represented as Veh_n), respectively, and d_n

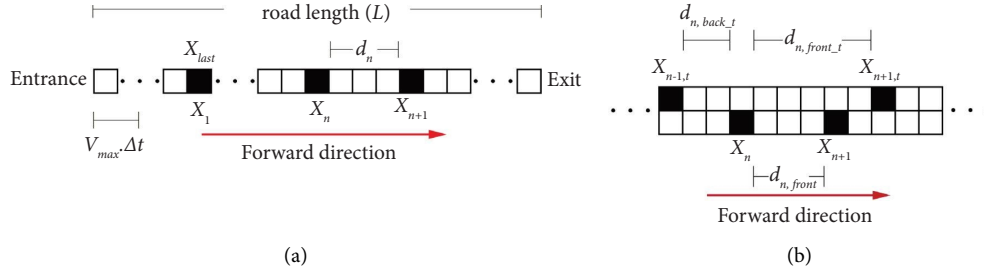


FIGURE 2: Schematic diagram of parameters in the update rules: (a) forward situation and (b) lane-changing situation.

refers to as the distance between Veh_n and the nearest vehicle (Veh_{n+1}) in front of it (see Figure 2(a)). Step 1 depicts the acceleration behavior of Veh_n for which the speed should not reach the maximum velocity (v_{max}) of vehicles, while Step 2 reflects the deceleration behavior of Veh_n to ensure that this vehicle is not hitting the vehicle in front of it. Step 3 represents the random deceleration behavior of Veh_n .

2.4.3. Lane Changing Rules. The lane changing rules on the two-lane main road (see Figure 2(b)) consist of two criteria as follows:

- (1) Incentive criterion as follows:

$$\begin{aligned}
 d_{n,front} &< \min((v_n + 1) \cdot \Delta t, v_{max} \cdot \Delta t) \text{ and } d_{n,front} < d_{n,front,t}, \\
 d_{n,front} &= x_{n+1} - x_n - l, \\
 d_{n,front,t} &= x_{n+1,t} - x_n - l.
 \end{aligned} \tag{5}$$

- (2) Safety criterion as follows:

$$\begin{aligned}
 d_{n,back,t} &> d_{safe,l}, \\
 d_{n,back,t} &= x_n - x_{n-1,t} - l.
 \end{aligned} \tag{6}$$

In equation (5), x_{n+1} and $x_{n+1,t}$ denote the positions of the preceding vehicles (Veh_{n+1}) on the same (as Veh_n) and target lanes, and $d_{n,front}$ and $d_{n,front,t}$ are the distances between Veh_n and Veh_{n+1} on the same lane as well as on the target lane, respectively. In equation (6), $d_{n,back,t}$ refers to as the distance between Veh_n and the vehicle behind it (Veh_{n-1}) on the target lane, with $x_{n-1,t}$ being the position of Veh_{n-1} , while $d_{safe,l}$ represents the safe distance of lane changing. The incentive criterion indicates the condition under which the front vehicle Veh_{n+1} on the same lane (as Veh_n) hinders the acceleration of Veh_n (i.e., due to the short distance of $d_{n,front}$), whereas the front vehicle Veh_{n+1} on the target lane provides the opportunity for Veh_n 's acceleration (i.e., given the relatively long distance of $d_{n,front,t}$). The safety criterion ensures the safety of Veh_n after changing lanes. If both the criteria are met, Veh_n will change lanes with the probability p_{lc} . It should be noted that lane changing rules only apply to vehicles on two-lane main roads.

2.4.4. Merging Rules. The merging rules are designed in accordance with the three collaborative merging strategies described in Section 2.3. Given the merging vehicle Veh_m on the acceleration lane, let L_m (1 or 0) be a parameter

indicating whether Veh_m merges into the main road. If $L_m = 1$, the vehicle will merge; otherwise, if $L_m = 0$, the vehicle will not merge. The value of L_m is determined based on the following procedure (see Algorithm 1):

If $L_m = 1$, Veh_m will merge into the main road. Note that the merging operation and corresponding rules are only applicable to merging vehicles on the acceleration lane.

3. Simulation and Discussion

In order to study the influence of the different merging strategies on on-ramp systems, we use the CA model to simulate the systems under four different situations (including no-strategies and strategies 1–3). The investigated on-ramp systems are divided into two cases, with case 1 for on-ramps having a one-lane main road while case 2 for those featured with a two-lane main road. Similar to most CA models, the length of each cell is 7.5 m and each vehicle occupies one cell (i.e., $l = 1$). The other parameters are set based on the commonly adopted values of the existing research, including the maximum velocity $v_{max} = 5$ cells/time step (i.e. 135 km/h) [3]; the road length $L = 2000$ cells and starting position x_{on} of the acceleration lane $x_{on} = L/2$ [9] (i.e., 1000 cells); the length of the acceleration lane $L_a = 5$ cells, randomization probability $p_s = 0.3$, lane-changing probability $p_{lc} = 0.8$ and safe distance of lane changing $d_{safe,l} = 2$ cells (i.e., 15 m) [34]. Moreover, the safe distance of merging vehicles and time step are $d_{safe,t} = 1$ cell (it will be discussed in Section 3.3) and $\Delta t = 1$ s, respectively.

```

(1) Initialization:  $L_m = 0$ ;
(2) Safety condition
  if ( $T_1^m \geq 0$  and  $T_2^m \geq 0$ ) {/No-Strategies
     $L_m = 1$ ;
  }else{
    merging strategies; //Strategies 1 or 2 or 3
  }
(3) Merging strategies
  Strategy 1:
  if ( $T_1^m \geq 0$  and  $T_2^m < 0$ ) {
    if ( $T_2^{m,front1} > 0$ ) {
       $v_{m,front1} = \min(v_{max}, v_{m,front1} + ((S_5^m - S_4^m)/\Delta t))$ 
      if ( $T_2^m \geq 0$ ) {
         $L_m = 1$ ;
      }
    }
  }
  Strategy 2:
  if ( $T_1^m < 0$  and  $T_2^m \geq 0$ ) {
    if ( $T_1^{m,back1} > 0$ ) {
       $v_{m,back1} = \max(0, v_{m,back1} - ((S_2^m - S_1^m)/\Delta t))$ 
      if ( $T_1^m \geq 0$ ) {
         $L_m = 1$ ;
      }
    }
  }
  Strategy 3:
  if ( $T_1^m < 0$  and  $T_2^m < 0$ ) {
    if ( $T_2^{m,front1} > 0$ ) {
       $v_{m,front1} = \min(v_{max}, v_{m,front1} + (S_5^m - S_4^m)/\Delta t)$ ;
    }
    if ( $T_1^{m,back1} > 0$ ) {
       $v_{m,back1} = \max(0, v_{m,back1} - (S_2^m - S_1^m)/\Delta t)$ ;
    }
    if ( $T_2^m \geq 0$  and  $T_1^m \geq 0$ ) {
       $L_m = 1$ ;
    }
  }

```

where as defined in Section 2.2, S_i^m ($i = 1, 2, 4, 5$) and T_j^m ($j = 1, 2$) are the elements of the traffic state array S^m and thread array T^m of Veh_m , while $v_{m,front1}$ and $v_{m,back1}$ are the speed of the nearest vehicles in front of and behind Veh_m ($Veh_{m,front1}$ and $Veh_{m,back1}$), respectively. Moreover, $T_2^{m,front1}$ and $T_1^{m,back1}$ denote the second and first elements of the thread array $T^{m,front1}$ and $T^{m,back1}$ of $Veh_{m,front1}$ and $Veh_{m,back1}$, respectively. Algorithm 1 in strategy 1 indicates that if $T_2^m < 0$, $Veh_{m,front1}$ should increase its speed in order to provide safe merging condition for Veh_m , with $(S_5^m - S_4^m)/\Delta t$ being the maximum acceleration of $Veh_{m,front1}$ in order to ensure its own safety (i.e., it will not collide with $Veh_{m,front2}$). Likewise, Algorithm 1 in strategy 2 requires that in the case of $T_1^m < 0$, $Veh_{m,back1}$ decreases its speed to provide merging condition for Veh_m , with $(S_2^m - S_1^m)/\Delta t$ being the maximum deceleration of $Veh_{m,back1}$ to guarantee its safety (i.e., it will not be hit by $Veh_{m,back2}$). Strategy 3 is the combination of the previous two strategies under the situation of $T_1^m < 0$ and $T_2^m < 0$, which suggests that both $Veh_{m,front1}$ accelerate and $Veh_{m,back1}$ decelerate to try to provide merging condition for Veh_m .

(4) Merging

ALGORITHM 1: The procedure for determining the value of L_m .

3.1. Average Velocity. We obtained the average velocity of vehicles under each of the situations with different values of vehicle entering probabilities a_1 (to the main road) and a_2 (to the ramp). Let \bar{v}_m and \bar{v}_r be the average velocity of vehicles on the main road (upstream) and on the ramp and Figures 3(a)–3(d) and 4(a)–4(d) present the values of \bar{v}_m and \bar{v}_r in relation to the threshold v_s ($v_s = 4.5$ cells/time step) (121.5 km/h) for case 1 and case 2, respectively. In these figures, the green, blue, red, and black scatters (denoted by I,

II, III, and IV) indicate the areas with (1) $\bar{v}_m > v_s$ and $\bar{v}_r > v_s$, (2) $\bar{v}_m > v_s$ and $\bar{v}_r < v_s$, (3) $\bar{v}_m < v_s$ and $\bar{v}_r > v_s$, and (4) $\bar{v}_m < v_s$ and $\bar{v}_r < v_s$, while the x -axis and y -axis represent the vehicle entering probabilities a_1 and a_2 , respectively.

From Figures 3(a)–3(d), it was observed that for the system with a one-lane main road (case 1), the merging strategies (Figures 3(b)–3(d)) can affect the velocity of vehicles on both the main road and ramp, when compared to no strategies (Figure 3(a)). Particularly, all the three

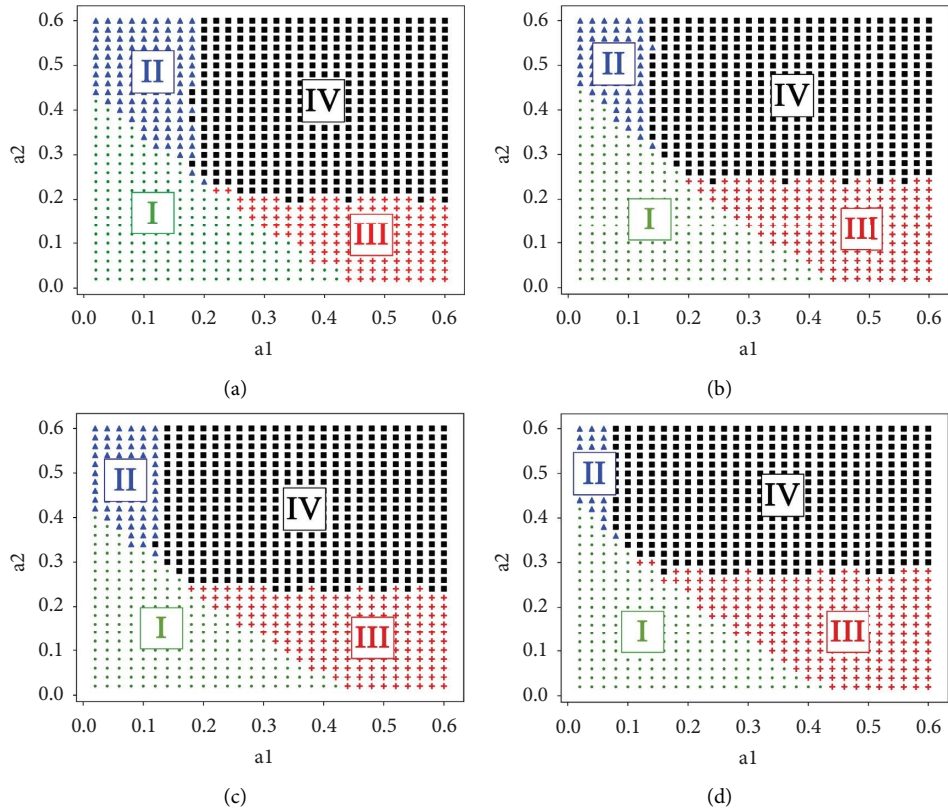


FIGURE 3: Schematic diagram of the relationship between the average velocity and threshold in the case of (a) no-strategies and (b–d) different merging strategies (strategies 1–3), case 1.

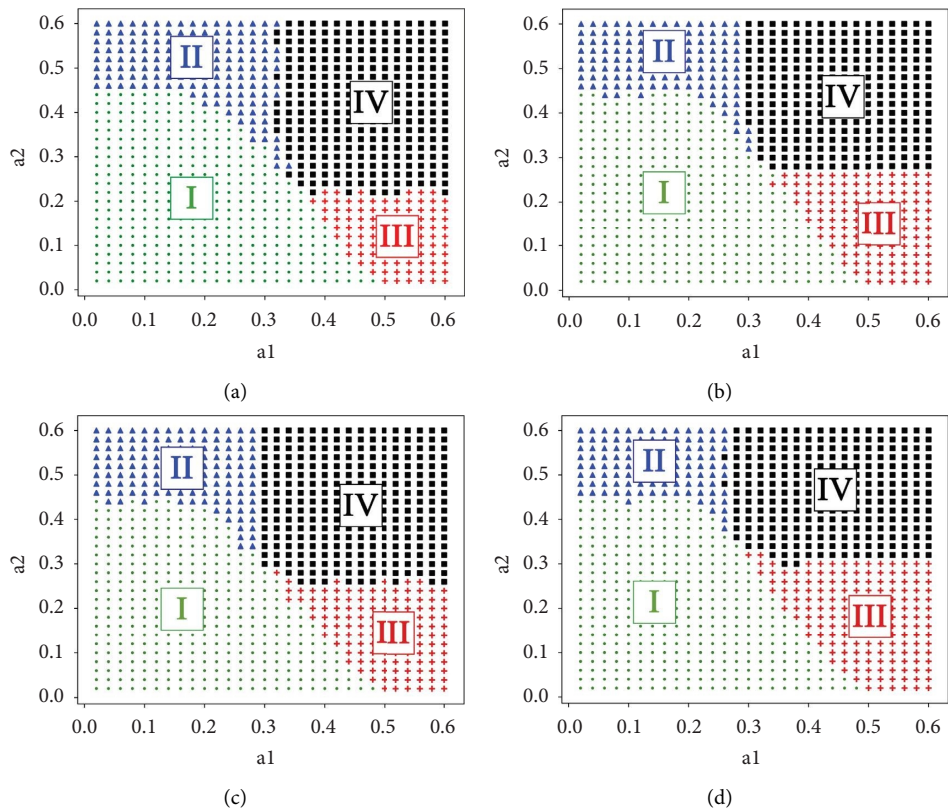


FIGURE 4: Schematic diagram of the relationship between average velocity and threshold in the case of (a) no-strategies and (b)–(d) different merging strategies (strategies 1–3), case 2.

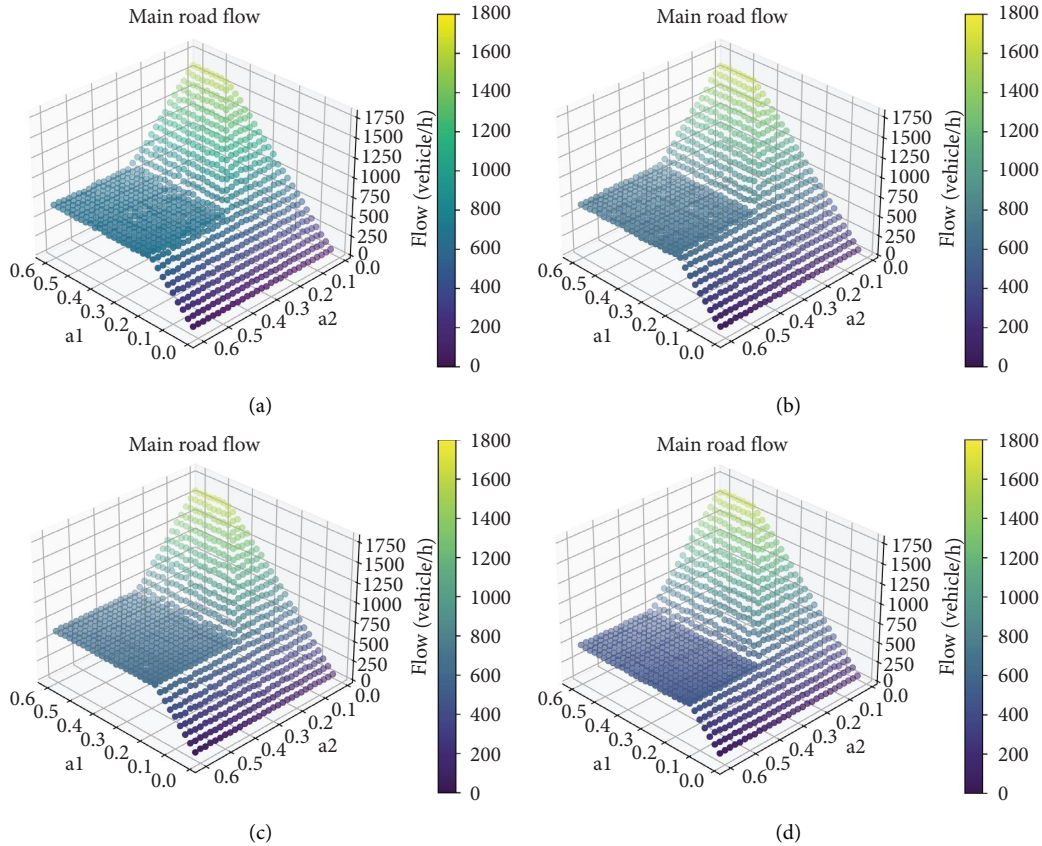


FIGURE 5: Upstream traffic flow rate of the main road in the case of (a) no-strategy and (b)–(d) different merging strategies (strategies 1–3), case 1.

strategies reduce the size of area II but increase that of area III, reflecting that there are less combined values of a_1 and a_2 for $\bar{v}_m > v_s$ and $\bar{v}_r < v_s$ but more for $\bar{v}_m < v_s$ and $\bar{v}_r > v_s$. This further suggests that in relation to no strategies, strategies 1–3 can decrease the average velocity of vehicles on the main road when a_1 and a_2 fall into the reduced-part-of-area-II, while improving that on the ramp if the two probabilities are in the increased-part-of-area-III. In addition, deviations also exist among individual strategies in terms of the size of the changed parts of the areas II and III. Strategy 3 has much larger sizes of these two changed parts than strategies 1 and 2, signifying that the former strategy can better improve the traffic efficiency of the ramp but at a higher cost of reducing that on the main road than the latter two strategies.

With respect to the system with a two-lane main road (case 2), the four areas (in Figures 4(a)–4(d)) display different sizes from the corresponding regions in case 1, particularly regarding areas I and IV which are much larger and smaller than those in case 1, respectively. This signifies that there are more combined values of a_1 and a_2 under which the average speed of vehicles on the main road and ramp is both high (i.e., $\bar{v}_m > v_s$ and $\bar{v}_r > v_s$), but less combinations of these two probabilities for which the speed of vehicles on the roads is low (i.e., $\bar{v}_m < v_s$ and $\bar{v}_r > v_s$). This can be attributed to the fact that vehicles on the main road (with two lanes) can change lanes and that the lane changing behavior has positive effect on the traffic

condition of the whole system and leads to the speed of vehicles on the roads higher. When the different situations within case 2 were compared, similar trends to those within case 1 were observed. Specifically, with reference to no strategies, all the three strategies reduce the size of area II but increase that of area III, signaling that these strategies reduce the average speed of vehicles on the main road when a_1 and a_2 are in the reduced-part-of-area-II while improving that on the ramp if a_1 and a_2 belong to the increased-part-of-area-III. Particularly, strategy 3 is featured with a much smaller size of area II but a larger size of area III, implying that this strategy significantly reduces the traffic efficiency of the main road but increases that on the ramp.

3.2. Flow Rate. In addition to speed, the impact of the merging strategies on traffic flow rate (i.e., the number of vehicles passing a reference point per hour) was also inspected. Let f_s and f_t be the average upstream flow rate on the main road in case 1 and case 2, respectively, while f_r be the flow rate on the ramp in both cases. Figures 5–10 visualize the evolution of the flow rates f_s , f_t , f_r , $f_s + f_r$, and $f_t + f_r$, respectively, under different situations with various combinations of a_1 and a_2 .

(Note: in Figure 7, in order to better display the changing trends of the z -variable, the x -axis and y -axis represent a_2

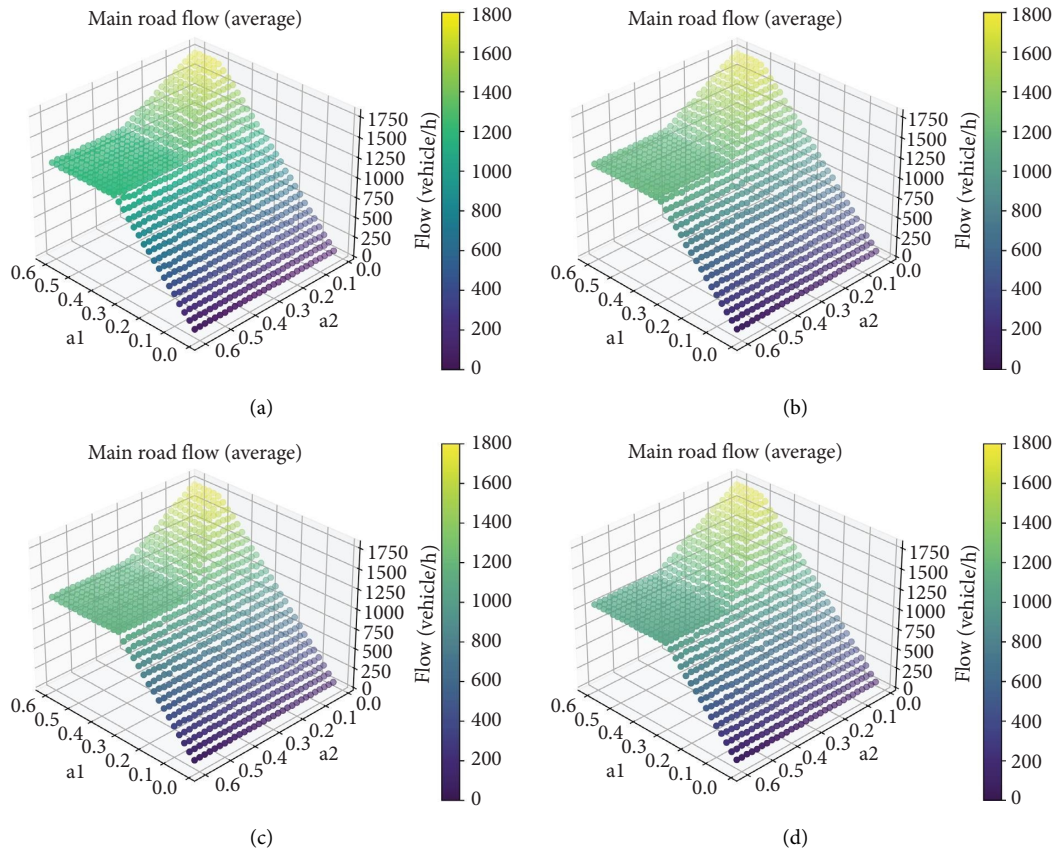


FIGURE 6: Upstream traffic flow rate of the main road in the case of (a) no-strategy and (b)–(d) different merging strategies (strategies 1–3), case 2.

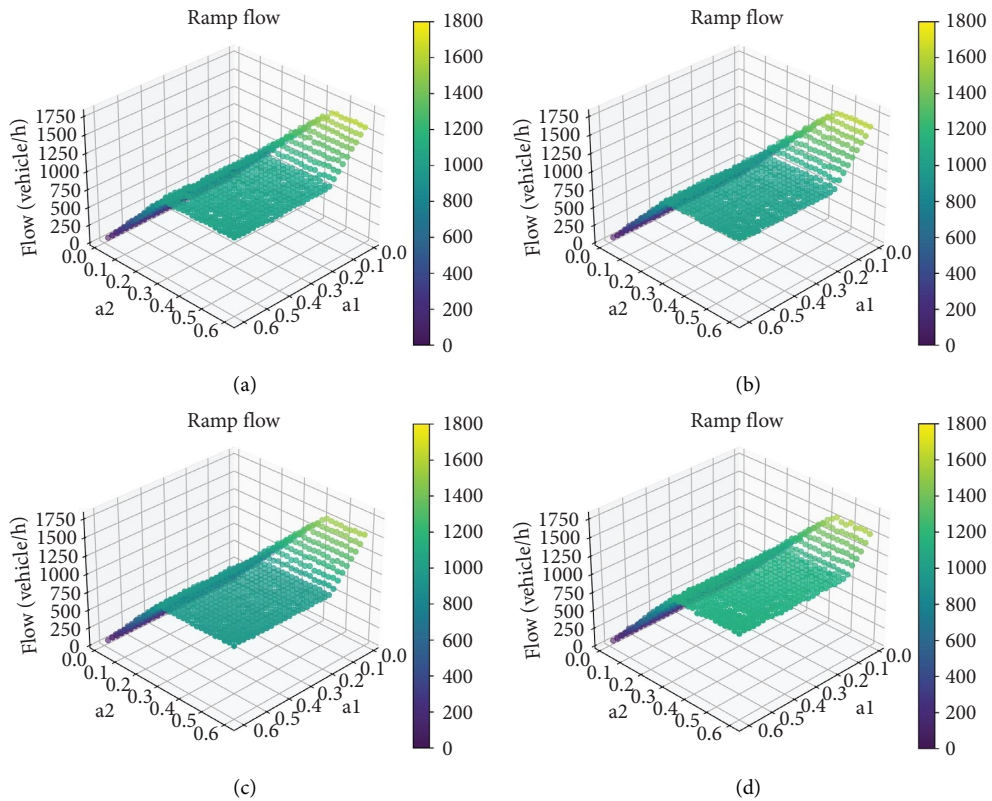


FIGURE 7: Traffic flow rate of ramp in the case of (a) no-strategy and (b)–(d) different merging strategies (strategies 1–3), case 1.

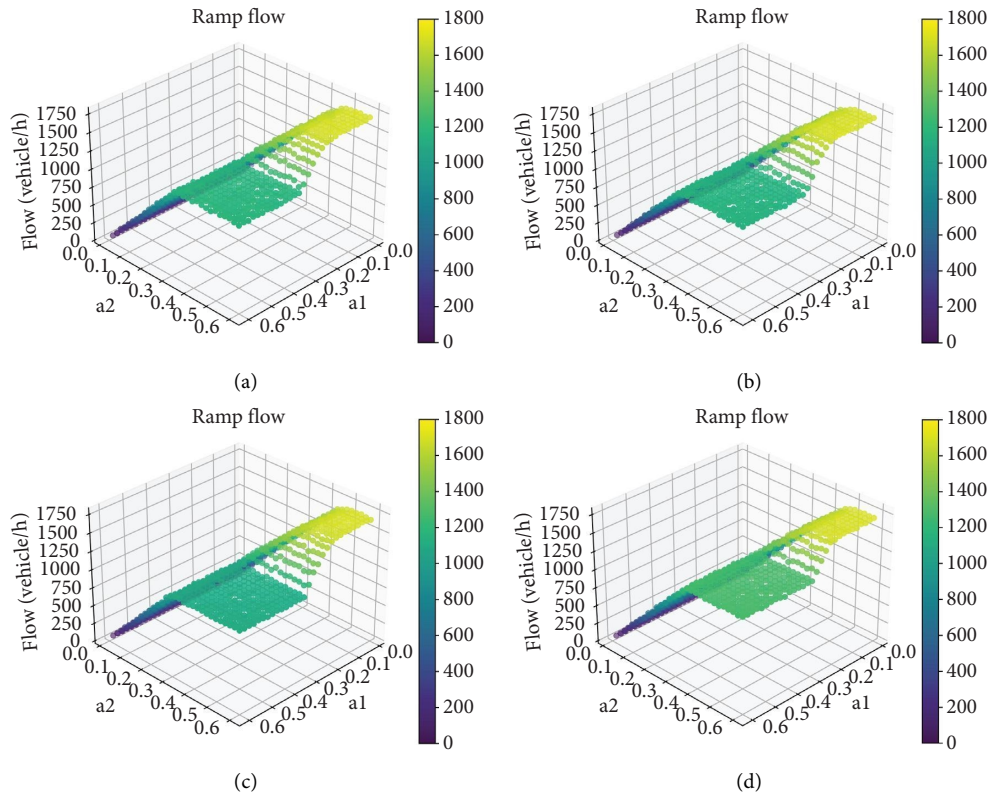


FIGURE 8: Traffic flow rate of ramp in the case of (a) no-strategy and (b)–(d) different merging strategies (strategies 1–3), case 2.

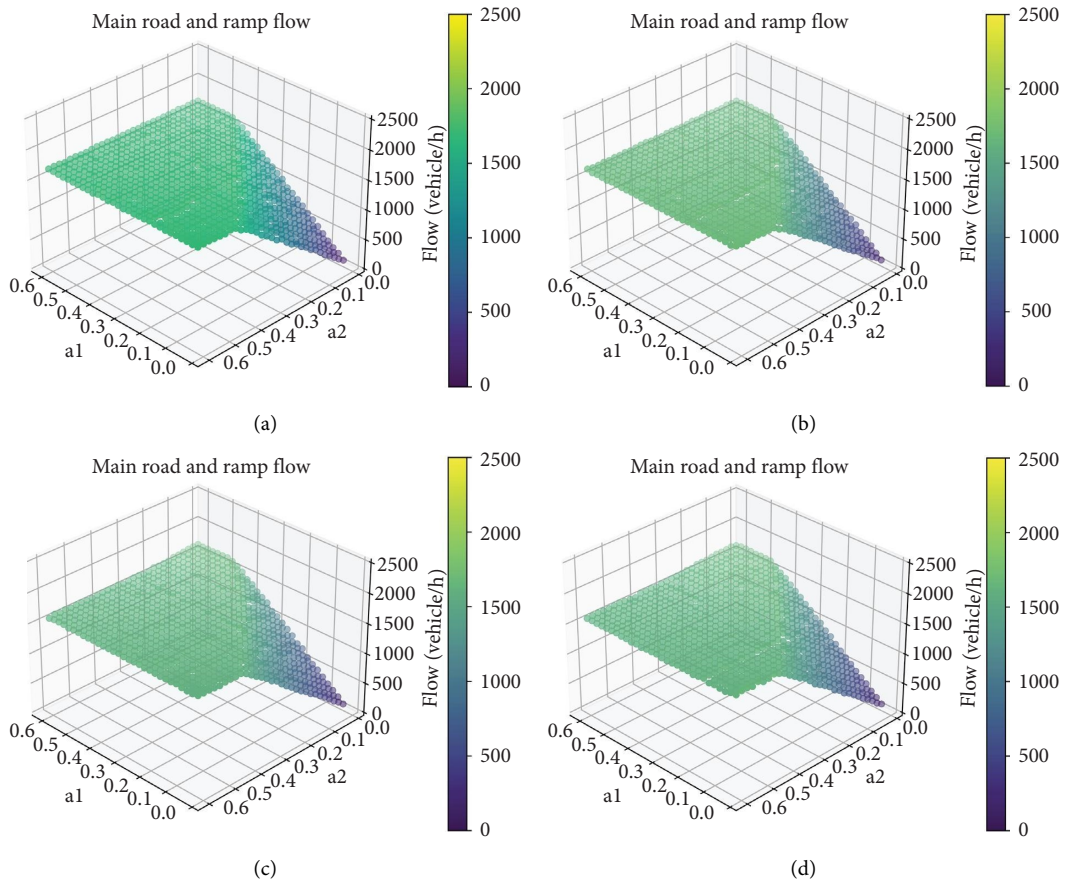


FIGURE 9: Traffic flow rate of main road and ramp in the case of (a) no-strategy and (b)–(d) different merging strategies (strategies 1–3), case 1.

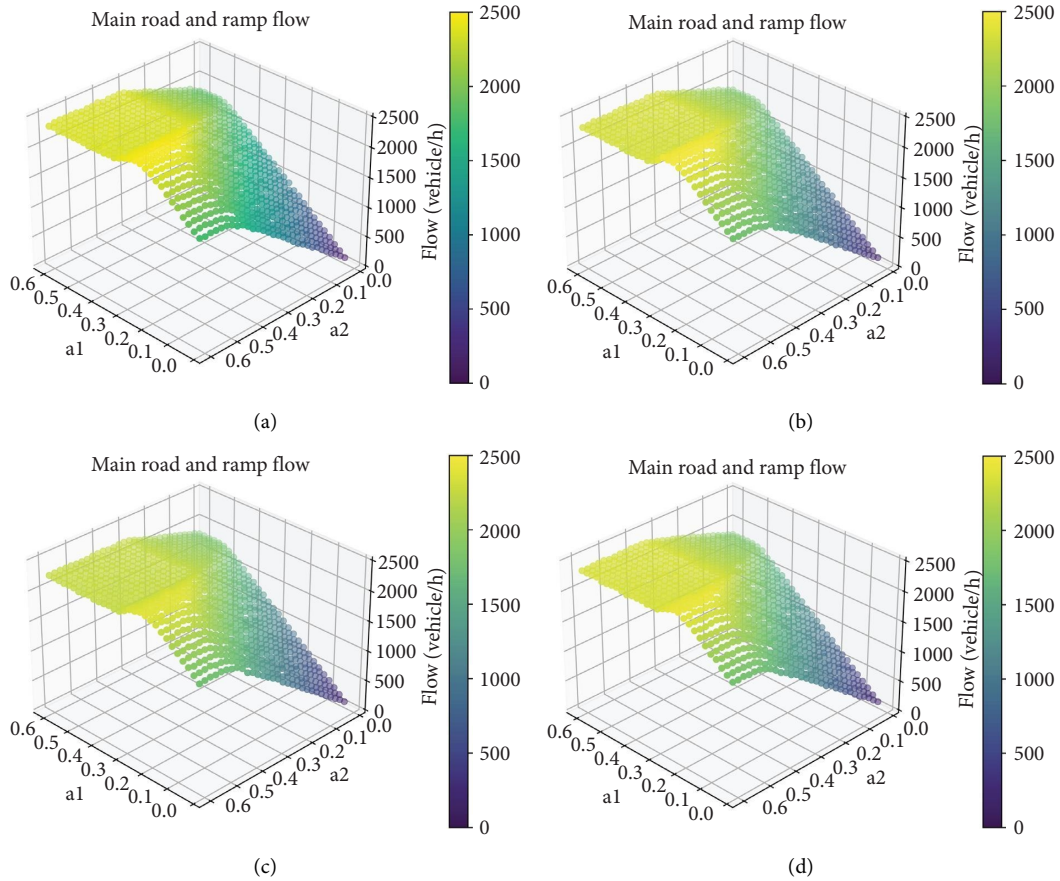


FIGURE 10: Traffic flow rate of main road and ramp in the case of (a) no-strategy and (b)–(d) different merging strategies (strategies 1–3), case 2.

and a_1 , respectively (instead of a_1 and a_2 in Figures 3–6). The same coordinate system is adopted in Figures 8 and 11).

From Figures 5(a)–5(d), it was noted that when a_2 is small (i.e., $a_2 \leq 0.28$), the flow rate f_s of the main road in case 1 shows no large differences between no-strategies and the other three strategies, with f_s reaching the largest value at $a_2 = 0$ in all these situations. This demonstrates that the merging strategies have little impact on f_s when the vehicle entering probability to the ramp is small. However, as a_2 increases ($a_2 > 0.28$), f_s begins to be affected by the strategies and displays a decreasing trend. However, this effect is not unlimited, manifested by the observation that f_s reduces until reaching a stable level (a “platform”). Moreover, the specific levels of the platforms vary among strategies, with strategy 1 having the highest level while strategy 3 displaying the lowest. This signifies that while all the strategies have a negative impact on the flow rate of the main road, strategy 3 causes the worst effect. A similar conclusion can be drawn for case 2 (in Figures 6(a)–6(d)), except that the threshold of a_2 which initiates the impact is higher ($a_2 > 0.32$). Moreover, the flow rate f_t and the stable levels for the “platform” in case 2 are significantly higher than those in case 1 due to the adoption of the additional lane on the main road.

Figures 7(a)–7(d) and 8(a)–8(d) depict the (positive) impact of the merging strategies on the flow rate f_r of the

ramp in case 1 and case 2, respectively, showing that when a_2 increases, f_r rises and reaches a stable level (a “platform”). This points out that while the merging strategies decrease the traffic flow on the main road, they increase that on the ramp. Moreover, similar to the decreasing effect on the main road, the increasing impact on the ramp is not boundless, making the flow rate rising until to a stable level.

Figures 9(a)–9(d) and 10(a)–10(d) visualize the flow rate over the whole on-ramp system (i.e., the main road and ramp), for case 1 (i.e., $f_s + f_r$), and case 2 (i.e., $f_t + f_r$), respectively. It was observed that $f_t + f_r$ is higher than $f_s + f_r$ at most combined values of a_1 and a_2 , especially when a_1 and a_2 are large. This suggests that it is more advantageous to set up a two-lane main road at merging sections. With respect to specific merging strategies, strategy 1 has almost no impact on $f_s + f_r$ or $f_t + f_r$, while strategy 2 reduces $f_s + f_r$ and $f_t + f_r$. In comparison, strategy 3 decreases $f_s + f_r$ but does not bring changes to $f_t + f_r$.

3.3. Effect of $d_{safe,t}$. Alongside the average velocity and flow rate, the effect of the merging safety distance parameter $d_{safe,t}$ on whole systems was further examined. In this process, we first simulated the system with $d_{safe,t} = 2$ cells (while the other parameters remaining the same as the original

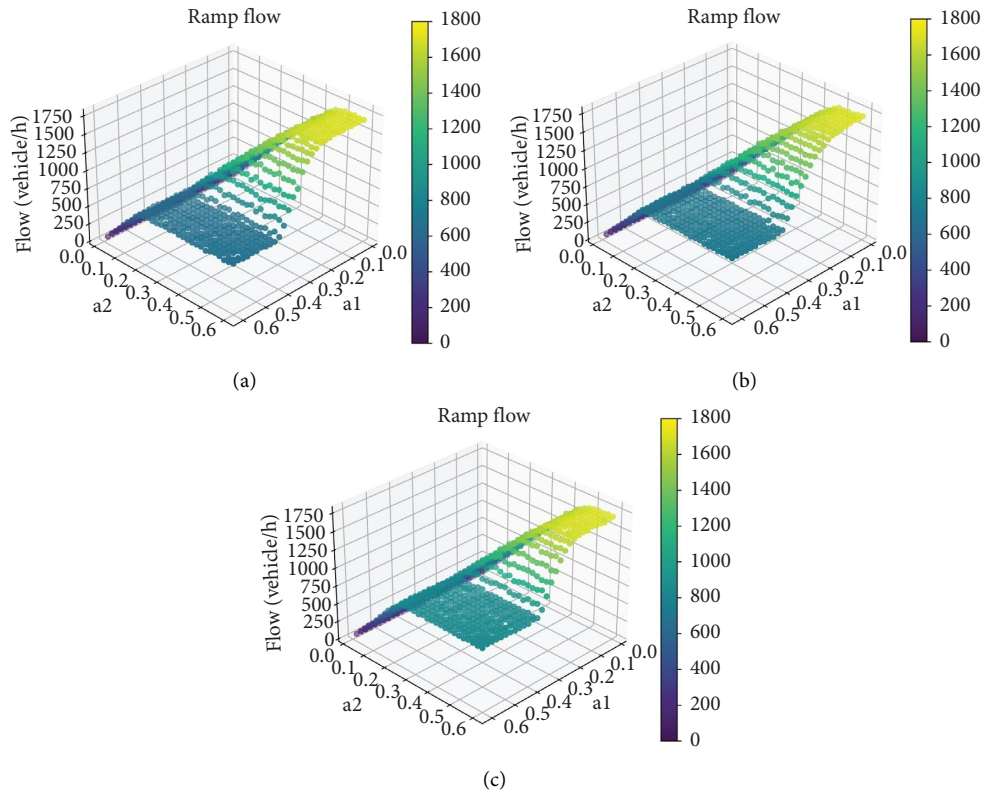


FIGURE 11: Traffic flow rate of the ramp with different strategies: ((a) strategy 1, (b) strategy 2, and (c) strategy 3), case 2, $d_{safe,t} = 2$.

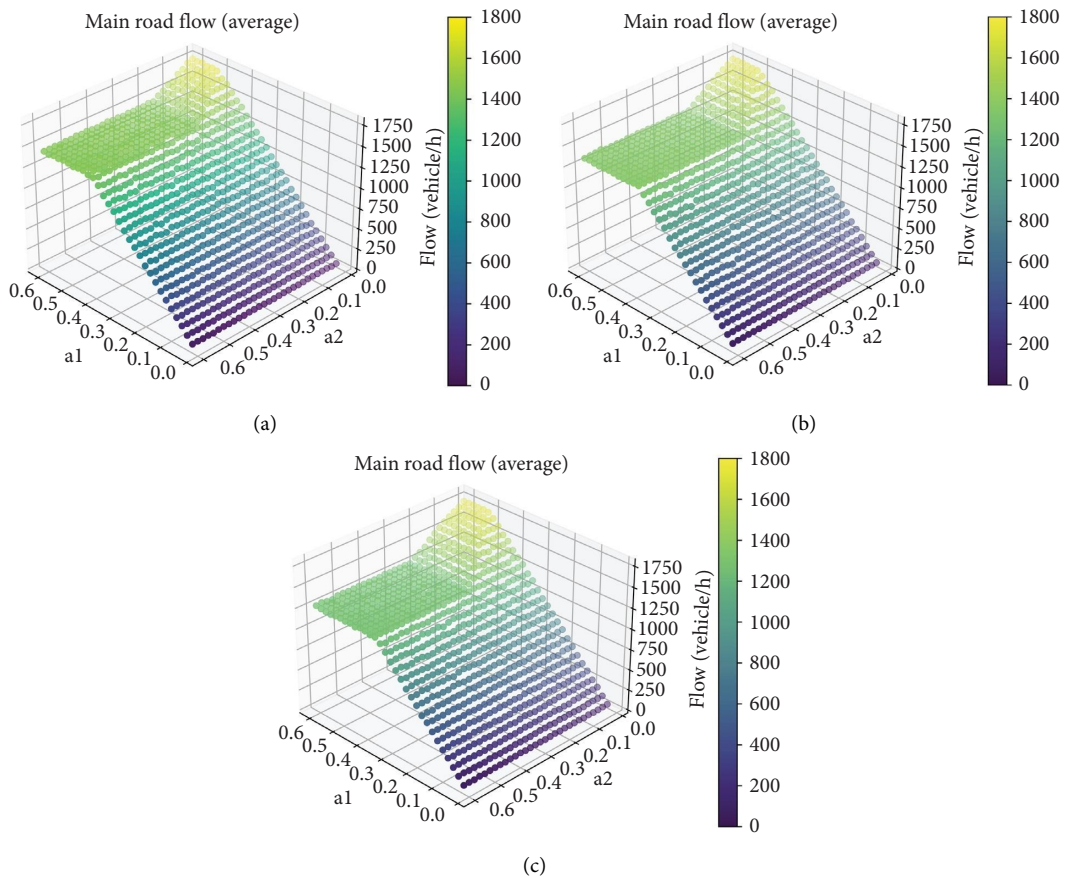


FIGURE 12: Traffic flow rate of the main road with different strategies: ((a) strategy 1, (b) strategy 2, and (c) strategy 3), case 2, $d_{safe,t} = 2$.

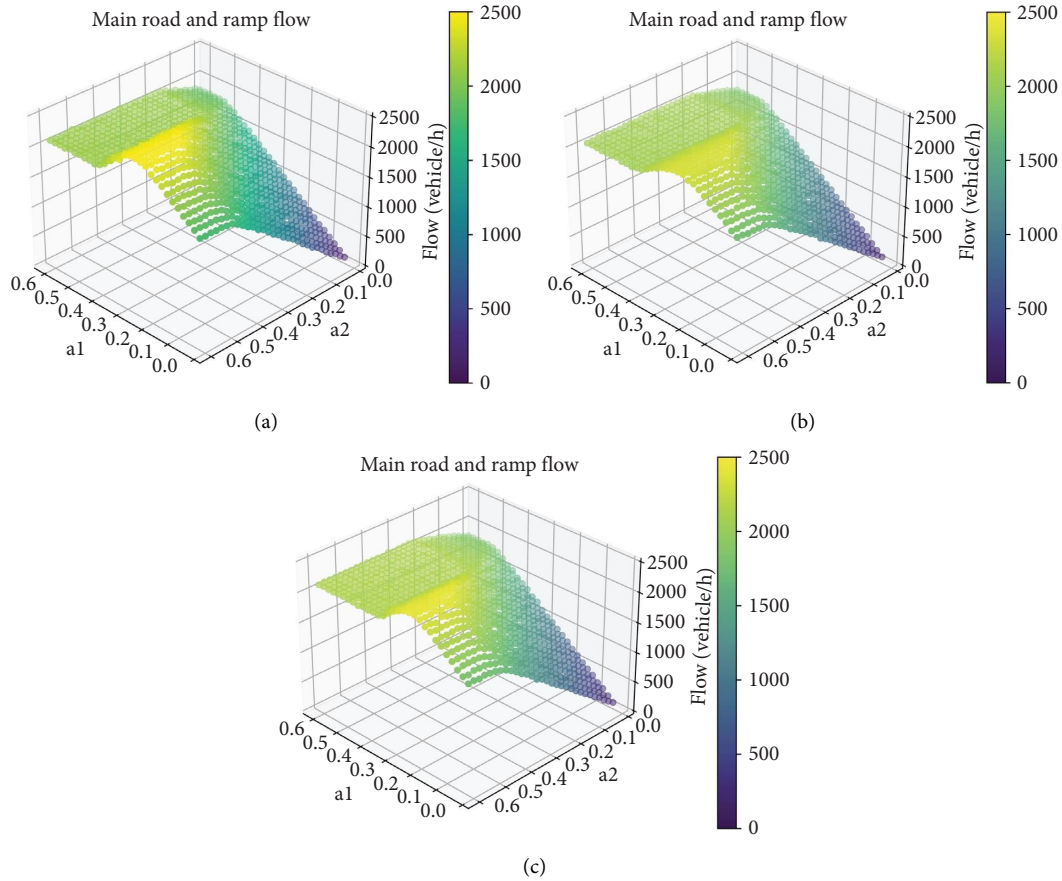


FIGURE 13: Traffic flow rate of the main road and ramp with different strategies: ((a) strategy 1, (b) strategy 2, and (c) strategy 3), case 2, $d_{\text{safe},t} = 2$.

simulation) and then, obtained the flow rate f_t , f_r , and $f_t + f_r$ for case 2. Figures 11–13 visualize the values of these variables. When these figures were compared with Figures 6(b)–6(d) 8(b)–8(d), and 10(b)–10(d) (with $d_{\text{safe},t} = 1$ cell in the original simulation), it shows that that when a_1 and a_2 are small, different values of $d_{\text{safe},t}$ have little effect on the flow of the on-ramp systems. However, when a_2 becomes large, the increase of $d_{\text{safe},t}$ will increase f_t , reduce f_r , and reduce $f_t + f_r$. Therefore, setting the merging safety distance parameter too large may lead to a negative impact on the whole system.

4. Conclusion

In this paper, we first defined traffic state arrays (S^m) and thread arrays (T^m) to represent the status of merging vehicles. We then summarized three major collaborative merging strategies and designed merging rules to express these strategies. Next, we analyzed the effect of these strategies on the speed and flow rate of on-ramp systems by means of CA simulation models. Finally, we examined the influence of the merging safety distance parameter ($d_{\text{safe},t}$) on the operation efficiency of the systems.

Based on this study, the following key results were obtained: (1) All the merging strategies give excessive

“priority” to the merging vehicle, leading to the reduction of average speed and flow rate of the main road. (2) Nevertheless, these strategies have a different effect on the entire system with a one-lane or two-lane main road. Due to lane-changing behavior, the system with a two-lane main road has more advantages than that featured with a one-lane main road, making the former system having higher operation efficiency than the latter under the same strategies. Thus, it is recommended that in an on-ramp system, a two-lane (even multiple-lane) main road should be considered. (3) The vehicles on the ramp and main road affect each other, and as the vehicle entering probabilities (a_1 and a_2) become large, the traffic flow rate on the main road decreases whereas that on the ramp increases. However, the effect is not unlimited. The flow rate on both roads finally reaches a stable level (forming a “platform”). (4) On the premise of ensuring safety, a small value of the merging safety distance parameter ($d_{\text{safe},t}$) should be adopted, as a large value would cause a considerable decrease in the flow rate of the whole system.

There are some limitations in this study, including the followings: (1) this study only considers three specific strategies, which is not complete, (2) the results derived through simulation should be further compared and verified with the experimental outcomes obtained from actual

situations, and (3) the impact of more forward and lane changing rules (in addition to the current ones depicted in Sections 2.4.2 and 2.4.3) on the results should be investigated. These drawbacks will be further addressed in the future research.

Data Availability

The simulation results can be obtained by contacting the author by e-mail.

Conflicts of Interest

The authors declare that they have no conflicts of interest.

Acknowledgments

This work was supported by the National Natural Science Foundation of China (Nos. 71621001, 72271021, and 71931002) and by the China Scholarship Council.

References

- [1] D. Helbing, "Traffic and related self-driven many-particle systems," *Reviews of Modern Physics*, vol. 73, no. 4, pp. 1067–1141, 2001.
- [2] P. G. Gipps, "A behavioural car-following model for computer simulation," *Transportation Research Part B: Methodological*, vol. 15, no. 2, pp. 105–111, 1981.
- [3] K. Nagel and M. Schreckenberg, "A cellular automaton model for freeway traffic," *Journal de Physique I*, vol. 2, no. 12, pp. 2221–2229, 1992.
- [4] B. S. Kerner and H. Rehborn, "Experimental features and characteristics of traffic jams," *Physical Review*, vol. 53, no. 2, pp. R1297–R1300, 1996.
- [5] B. S. Kerner and H. Rehborn, "Experimental properties of complexity in traffic flow," *Physical Review*, vol. 53, no. 5, pp. R4275–R4278, 1996.
- [6] J.-W. Zeng, Y.-S. Qian, S.-B. Yu, and X.-T. Wei, "Research on critical characteristics of highway traffic flow based on three phase traffic theory," *Physica A: Statistical Mechanics and Its Applications*, vol. 530, Article ID 121567, 2019.
- [7] J. Zeng, Y. Qian, P. Mi et al., "Freeway traffic flow cellular automata model based on mean velocity feedback," *Physica A: Statistical Mechanics and Its Applications*, vol. 562, Article ID 125387, 2021.
- [8] X. Li, S. Qu, and Y. Xia, "Cooperative lane-changing rules on multilane under condition of cooperative vehicle and infrastructure system, in Chinese," *China Journal of Highway and Transport*, vol. 27, 2014.
- [9] R. Jiang, B. Jia, and Q.-S. Wu, "The stochastic randomization effect in the on-ramp system: single-lane main road and two-lane main road situations: single-lane main road and two-lane main road situations," *Journal of Physics A: Mathematical and General*, vol. 36, no. 47, pp. 11713–11723, 2003.
- [10] J. Zeng, Y. Qian, Z. Lv et al., "Expressway traffic flow under the combined bottleneck of accident and on-ramp in framework of Kerner's three-phase traffic theory," *Physica A: Statistical Mechanics and Its Applications*, vol. 574, Article ID 125918, 2021.
- [11] B. Jia, R. Jiang, and Q.-S. Wu, "The effects of accelerating lane in the on-ramp system," *Physica A: Statistical Mechanics and Its Applications*, vol. 345, no. 1-2, pp. 218–226, 2005.
- [12] L. Xin-Gang, G. Zi-You, J. Bin, and J. Rui, "Traffic dynamics of an on-ramp system with a cellular automaton model," *Chinese Physics B*, vol. 19, no. 6, Article ID 060501, 2010.
- [13] B. Ran, S. Leight, and B. Chang, "A microscopic simulation model for merging control on a dedicated-lane automated highway system," *Transportation Research Part C: Emerging Technologies*, vol. 7, no. 6, pp. 369–388, 1999.
- [14] Z. Sun, T. Huang, and P. Zhang, "Cooperative decision-making for mixed traffic: a ramp merging example," *Transportation Research Part C: Emerging Technologies*, vol. 120, 2020.
- [15] T.-Q. Tang, J.-G. Li, S.-C. Yang, and H.-Y. Shang, "Effects of on-ramp on the fuel consumption of the vehicles on the main road under car-following model," *Physica A: Statistical Mechanics and Its Applications*, vol. 419, pp. 293–300, 2015.
- [16] M. Sarvi and M. Kuwahara, "Using ITS to improve the capacity of freeway merging sections by transferring freight vehicles," *IEEE Transactions on Intelligent Transportation Systems*, vol. 9, no. 4, pp. 580–588, 2008.
- [17] R. Scarinci and B. Heydecker, "Control concepts for facilitating motorway on-ramp merging using intelligent vehicles," *Transport Reviews*, vol. 34, no. 6, pp. 775–797, 2014.
- [18] Y. Zhou, E. Chung, A. Bhaskar, and M. E. Cholette, "A state-constrained optimal control based trajectory planning strategy for cooperative freeway mainline facilitating and on-ramp merging maneuvers under congested traffic," *Transportation Research Part C: Emerging Technologies*, vol. 109, pp. 321–342, 2019.
- [19] Y. Liu, J. Guo, J. Taplin, and Y. Wang, "Characteristic analysis of mixed traffic flow of regular and autonomous vehicles using cellular automata," *Journal of Advanced Transportation*, vol. 2017, Article ID 8142074, 10 pages, 2017.
- [20] Y. Qian, J. Zeng, N. Wang, J. Zhang, and B. Wang, "A traffic flow model considering influence of car-following and its echo characteristics," *Nonlinear Dynamics*, vol. 89, no. 2, pp. 1099–1109, 2017.
- [21] J. Zeng, Y. Qian, F. Yin, L. Zhu, and D. Xu, "A multi-value cellular automata model for multi-lane traffic flow under Lagrange coordinate," *Computational & Mathematical Organization Theory*, vol. 28, no. 2, pp. 178–192, 2021.
- [22] M. Tanveer, F. A. Kashmiri, H. Yan, T. Wang, and H. Lu, "A cellular automata model for heterogeneous traffic flow incorporating micro autonomous vehicles," *Journal of Advanced Transportation*, vol. 2022, Article ID 8815026, 21 pages, 2022.
- [23] B. Jia, R. Jiang, Q.-S. Wu, and M.-b. Hu, "Honk effect in the two-lane cellular automaton model for traffic flow," *Physica A: Statistical Mechanics and Its Applications*, vol. 348, pp. 544–552, 2005.
- [24] X.-C. Shang, X.-G. Li, D.-F. Xie, B. Jia, and R. Jiang, "Two-lane traffic flow model based on regular hexagonal cells with realistic lane changing behavior," *Physica A: Statistical Mechanics and Its Applications*, vol. 560, Article ID 125220, 2020.
- [25] P. Wagner, K. Nagel, and D. E. Wolf, "Realistic multi-lane traffic rules for cellular automata," *Physica A: Statistical Mechanics and Its Applications*, vol. 234, no. 3-4, pp. 687–698, 1997.
- [26] Y. Qian, J. Luo, J. Zeng, X. Shao, and W. Guo, "Study on security features of freeway traffic flow with cellular automata model—taking the number of overtake as an example," *Measurement*, vol. 46, no. 6, pp. 2035–2042, 2013.
- [27] E. G. Campari and G. Levi, "A cellular automata model for highway traffic," *The European Physical Journal B*, vol. 17, no. 1, pp. 159–166, 2000.

- [28] R. Jiang, Q. S. Wu, and B. H. Wang, "Cellular automata model simulating traffic interactions between on-ramp and main road," *Physical Review*, vol. 66, no. 3, Article ID 036104, 2002.
- [29] G. Diedrich, L. Santen, A. Schadschneider, and J. Zittartz, "Effects of on- and off-ramps in cellular automata models for traffic flow," *International Journal of Modern Physics C*, vol. 11, no. 2, pp. 335–345, 2000.
- [30] V. Milanés, J. Godoy, J. Villagra, and J. Perez, "Automated on-ramp merging system for congested traffic situations," *IEEE Transactions on Intelligent Transportation Systems*, vol. 12, no. 2, pp. 500–508, 2011.
- [31] T. Awal, L. Kulik, and K. Ramamohanrao, "Optimal traffic merging strategy for communication- and sensor-enabled vehicles," in *Proceedings of the 16th International IEEE Annual Conference on Intelligent Transportation Systems (ITSC 2013)*, The Hague, Netherlands, October 2013.
- [32] C. Letter and L. Elefteriadou, "Efficient control of fully automated connected vehicles at freeway merge segments," *Transportation Research Part C: Emerging Technologies*, vol. 80, pp. 190–205, 2017.
- [33] Ca, "C.E. F cellular automata," Academic Press, New York, NY, USA, 1968.
- [34] X.-G. Li, B. Jia, Z.-Y. Gao, and R. Jiang, "A realistic two-lane cellular automata traffic model considering aggressive lane-changing behavior of fast vehicle," *Physica A: Statistical Mechanics and Its Applications*, vol. 367, pp. 479–486, 2006.